ELSEVIER

Journal of Chromatography A, 744 (1996) 63–74

JOURNAL OF CHROMATOGRAPHY A

Capillary electrochromatography – a high-efficiency micro-separation technique

Monika M. Dittmann, Gerard P. Rozing*

Hewlett-Packard GmbH, Waldbronn Analytical Division, P.O. Box 1280, D-76337 Waldbronn, Germany

Abstract

Capillary electrochromatography (CEC) is a novel separation technique in which mobile phase transport through a capillary (50–200 μm I.D.) packed with stationary phase particles is achieved by electroosmotic flow (EOF) instead of a pressure gradient as in HPLC. Electroosmotic flow allows the usage of smaller particles and longer columns than in HPLC because of the absence of backpressure. Separation is achieved by partitioning between mobile and stationary phase and—in the case of charged analytes—by differential electrophoretic mobilities. In the reversed-phase mode, capillary electrochromatography has the potential to yield efficiencies five to ten times higher than standard RP-HPLC. For this reason CEC has started to create high interest among chromatographers. This paper will discuss the theoretical background of CEC, demonstrate the feasibility of CEC as a high-efficiency reversed-phase separation technique, compare theoretically achievable results to those obtained in practice and present fundamental studies on operational parameters such as dependence of EOF and efficiency on pH and organic modifier content.

Keywords: Electrochromatography; Buffer composition; Hydroxybenzoates; Polynuclear aromatic hydrocarbons

1. Introduction

In the past few years, capillary electroseparation methods such as capillary zone electrophoresis (CZE), micellar electrokinetic capillary chromatography (MECC) and capillary gel electrophoresis (CGE) have found widespread use in the analytical laboratory.

These separations are generally performed using aqueous buffer systems in fused-silica (FS) capillaries of 25–100 μm I.D. with an electric field of about 300 V/cm applied to the column in axial direction. Solutes are transported through the column by electromigration and/or electroosmotic flow (EOF). EOF is generated due to the electrical double layer which exists at all solid–liquid interfaces. The flow velocity is independent of the capillary diameter or, in case of packed FS capillaries, of the particle diameter. The ideal EOF velocity profile is plug like, i.e., there is no flow velocity gradient across the column.

Capillary electrochromatography, CEC, is carried out in FS-tubes of 50–100 μm I.D. packed with small (typically 3 μm and smaller) silica based particles. Eluents are composed of aqueous buffers mixed with organic modifiers (e.g., acetonitrile). Under these conditions an electroosmotic flow of up to 3 mm/s is generated. Neutral solutes are separated by partitioning between mobile and stationary phase while moving through the column with the EOF as in liquid chromatography. Charged solutes have an additional electrophoretic mobility in the applied

*Corresponding author.

0021-9673/96/$15.00
PII S0021-9673(96)00382-2

electric field. In CEC separation is achieved by the combined effects of electrophoresis and partitioning. In this paper we will only deal with neutral analytes and therefore with mere chromatographic aspects of the technique.

Pretorius et al. [1] have already in 1974 demonstrated the possibility of using EOF as a means to transport liquid through a chromatographic column but only recently an increasing number of publications [2–14] deal with theoretical and practical aspects of CEC.

In the following article we will discuss the theoretical aspects of CEC, compare efficiencies achieved in practice with those predicted by theory and discuss the influence of operational parameters such as pH, amount and nature of organic modifier on EOF velocity and separation.

2. Theoretical aspects

2.1. Electroosmotic flow in a packed capillary

In CEC the transport of mobile phase through the column is achieved by electroosmotic flow (EOF) instead of pressure driven flow as in standard HPLC. The origin of this flow is the electrical double layer that is formed at the solid–liquid interface of a charged surface in contact with an electrolyte solution. In a capillary packed with silica particles the surfaces of the capillary wall and of the particles are negatively charged due to the dissociation of silanol groups. The electrical double layer in this case contains an excess of mobile positive ions. When an axial electrical field is applied to the column these ions migrate towards the cathode moving the bulk solution by viscous drag. An illustration is given in Fig. 1. EOF differs from pressure driven laminar flow in three important aspects: (a) it has a plug flow profile (no cross-sectional flow velocity differences like in hydraulic flow), (b) in channels between 0.1 μm and ca. 150 μm the linear EOF velocity is independent of the channel width and (c) no column back pressure is generated.

The velocity of this flow depends on the surface charges of the capillary wall and the particles as well as on the properties of the eluent. It can be assumed that in packed capillaries the influence of the wall on the total EOF is very small due to its small relative surface area.

The Smoluchowski equation gives the velocity of the EOF as

$$u_{eo} = \frac{\epsilon_0 \epsilon_r \zeta E}{\eta} \tag{1}$$

where ϵ_0 is the permittivity of vacuum, ϵ_r is the dielectric constant of the eluent, ζ is the zeta potential, η is the viscosity of the eluent and E is the electric field strength.

For small potentials, the ζ potential can be expressed as [15]

$$\zeta = \frac{\sigma}{\epsilon_0 \epsilon_r \kappa} \tag{2}$$

where σ is the charge density at the surface of shear and κ is the Debye–Hückel parameter; for a strong

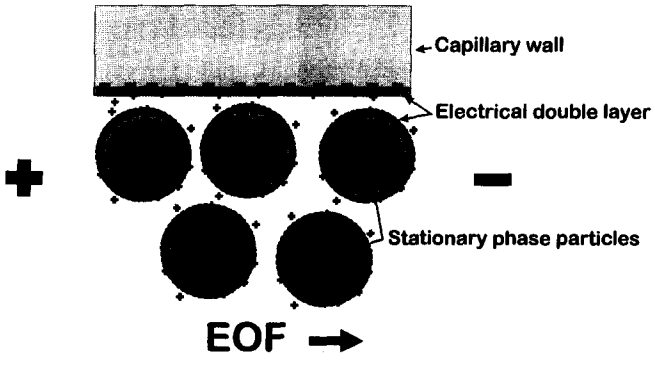

Fig. 1. Origin of electroosmotic flow (EOF) in a packed capillary.

monovalent electrolyte $\kappa = \left[\frac{2cF^2}{\epsilon_0\epsilon_r RT}\right]^{1/2}$. Combining of Eqs. 1 and 2 yields

$$u_{eo} = \frac{\sigma\left[\frac{\epsilon_0\epsilon_r RT}{2cF^2}\right]^{1/2} E}{\eta} \quad (3)$$

The EOF velocity depends such on surface charge density, dielectric constant, buffer ionic strength, eluent viscosity and temperature. For open tubular fused-silica capillaries the ζ potential has been determined to be between 20 and 120 mV depending on pH [21]. The ζ potential in capillaries made of polymeric materials (polytetrafluorethylene, polyethylene or polyvinylchloride) ranges from 0 mV at pH 2 to ca. 60 mV at pH 10 [20]. For C_{18} derivatized particles the ζ potential can be assumed to be in the same range as that of polymeric materials.

If we assume $\zeta = 40$ mV, $\epsilon_0 = 80$ and $\eta = 0.89$ cP, we obtain from Eq. 1 linear EOF velocities between 0.3 mm/s at 100 V/cm and 3.2 mm/s at 1000 V/cm.

Fig. 2 shows the velocities actually achieved on a C_{18} packing material (CEC Hypersil C_{18}, 3 μm) vs. electric field strength. Depending on buffer pH and surface charge of the packing particles linear flow-rates of up to 2.5 mm/s on columns with a total length of 35 cm have been achieved in our studies. This flow-rate range is comparable to the operation range for HPLC columns.

2.2. Zone broadening in CEC vs. HPLC

To estimate the effect that operation of a column with EOF instead of pressure drive would have on the efficiency of a separation, we adopted Horvaths model [16,17] for HPLC and modified it to account for the effects of EOF. The details of this treatment have been published [18]. As Horvath, we assumed that the HETP equation can be expressed as the sum of independent terms, that account for the different contributions to zone broadening.

$$H = H_{disp.} + H_{e,diff.} + H_{i,diff.} + H_{t,diff.} + H_{kin.} \quad (4)$$

$H_{disp.}$ is the plate height increment due to axial dispersion of the solute in the interstitial space, $H_{e,diff.}$ is the plate height increment caused by film resistance at the particle boundary, $H_{i,diff.}$ is the plate height contribution from intraparticle diffusion, $H_{t,diff.}$ is the contribution from transchannel mass transfer and $H_{kin.}$ the contribution of solute interaction kinetics with the stationary phase.

In packed columns, dispersion in the axial is given by Eq. 5.

$$H_{disp.} = H_{a,diff} + H_{eddy,diff.} \quad (5)$$

Here $H_{a,diff.}$ is the plate height contribution due to static diffusion in axial direction and $H_{eddy,diff.}$ is the

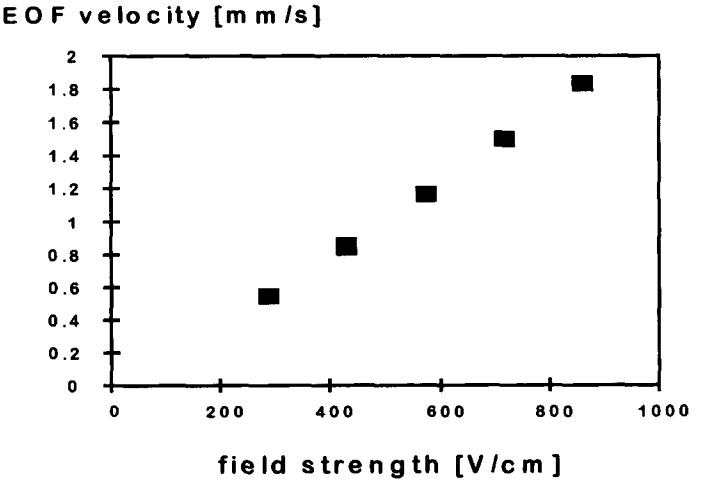

Fig. 2. Plot of EOF velocity vs. the applied electric field strength. Conditions: 250(335) mm×0.1 mm CEC Hypersil C_{18}, 2.5 μm, acetonitrile–MES 25 m*M* pH 6 (80:20), 10 bar pressure applied to both ends of capillary, 20°C.

contribution due to the flow velocity differences (eddy diffusion).

Of all the terms that contribute to zone broadening, only eddy diffusion $H_{eddy,diff}$ and transchannel diffusion $H_{t,diff}$ depend on the type of flow profile in the column. The transchannel diffusion term accounts for the fact that a solute has to diffuse through the channels between the particles in order to reach the stationary phase. Due to the plug like flow velocity profile the contribution of transchannel diffusion is smaller in an EOF driven system than in a pressure driven system. In a packed column, however, the contribution of the transchannel diffusion term to the total HETP value is very small as the diameter of channels are small (ca. 1/3 of the particle size).

The magnitude of the eddy diffusion term depends on the differences in flow velocity in the channels between the particles (an illustration is given in Fig. 3). The velocity of pressure driven flow varies with the diameter of the channels. Solutes may find fast and slow flow paths through the column, resulting in overall zone dispersion. In an electrically driven system, the flow velocity is largely independent on the channel width (see Fig. 3), such that solutes changing from one channel to the other do not experience a change in flow velocity resulting in much lower zone dispersion.

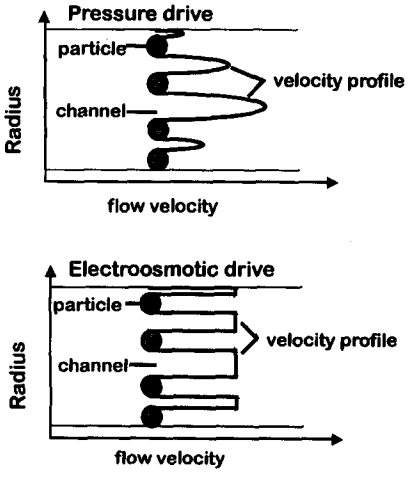

Fig. 3. Diagram of flow velocity profiles vs. channel diameter for pressure driven (top) and electroosmotically driven (bottom) flow.

Fig. 4 shows the HETP values as a function of linear velocity calculated from our model [18] for a column packed with 5 μm particles operated with laminar (pressure) flow (top) compared to a column operated with EOF (bottom). The figures show the total HETP curves, the contributions from terms that are independent on flow profile, the contributions from transchannel diffusion and the contributions from Eddy diffusion.

It can be seen that the difference in the transchannel diffusion term is negligibly small. The eddy diffusion term shows however a large difference resulting in a reduction of the HETP value by a factor of ca. 2 for an EOF driven system (in the minimum of the H–u curve).

This means that a column packed with 5 μm particles operated with EOF would be twice as efficient as a column operated with pressure flow. The use of EOF becomes even more advantageous when the particle size is reduced. Although the difference in eddy diffusion becomes smaller with

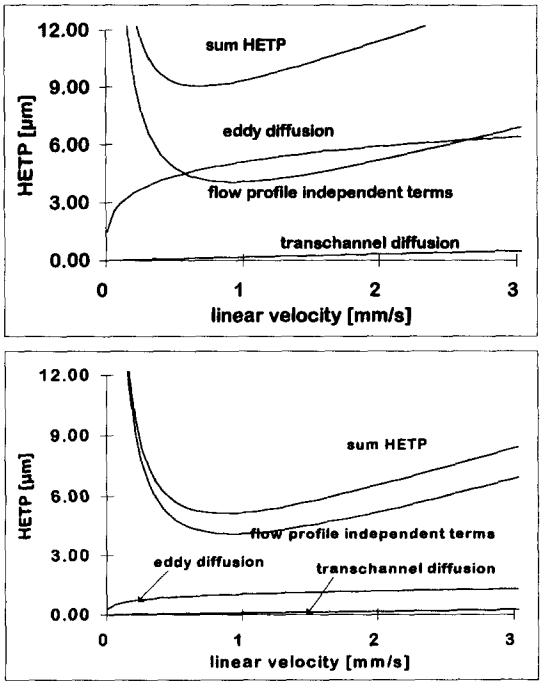

Fig. 4. Plots of HETP vs. u for HPLC (top) and CEC (bottom) for 5 μm particles. Plots are calculated for an analyte with $k'=5$ and a diffusion coefficient of $1.5 \cdot 10^{-5}$ cm^2/s.

smaller particle size, the fact that EOF does not generate column back pressure plays an important role when reducing particle size.

When operational constraints of maximum pressure in HPLC (400 bar) and voltage in CEC (30 kV) are taken into account, the achievable efficiencies with both techniques can be estimated. This was done in the following way. For a given column length we calculate the flow velocity that is achievable under the given operational constraints according to

$$u_{max} = \frac{V_{max}\epsilon_0\epsilon_r\zeta}{L\eta} \quad (6)$$

$$u_{max} = \frac{\Delta P_{max} d_p^2 \Phi}{L\eta} \quad (7)$$

In our calculations we assume 40 mV for the ζ potential and 1000 for the column resistance factor ϕ, $\epsilon_r = 80$, $\eta = 0.89$ cP (water).

For u_{max} we then calculate the plate number from our HETP model and the analysis time for a component with a $k' = 5$. The results for a 3 μm packing material are shown in Fig. 5. The straight line corresponds to an analysis time of 25 min. In HPLC this analysis time is obtained for a 30 cm long column which would yield ca. 50 000 plates. Increasing the analysis time to 50 min (45 cm column) would result in a plate number of 75 000. In CEC, an analysis time of 25 min could be obtained on a 50 cm long column, which would yield ca. 150 000 plates. Here an increase in analysis time to 50 min (70 cm column) would yield a plate number of 220 000. When using smaller packing materials (<2 μm) the benefit of CEC is even more pronounced.

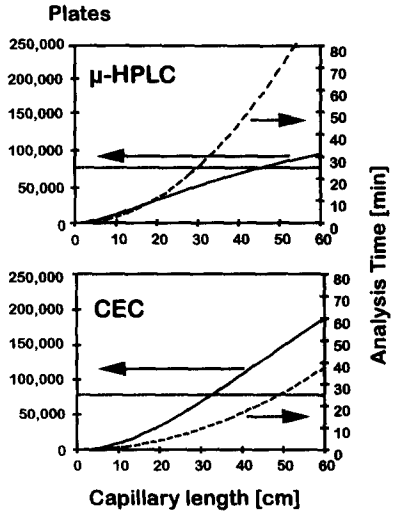

Fig. 5. Plots of analysis time (dashed curve) and plate number vs. column length for μ-HPLC (top) and CEC (bottom). The two curves in each plot show the number of achievable plates and the analysis time for maximum operating pressure (400 bar) and voltage (30 kV) calculated from our HETP model as a function of column length. Analysis time is for an analyte with $k' = 5$. The straight line represents an analysis time of 25 min. Details of the calculation are given in the text.

Table 1
Theoretically achievable plates per column for different particle sizes in capillary HPLC and CEC

Particle size	Capillary HPLC		CEC	
	length	N/column	length	N/column
5 μm	50 cm	45 000	50 cm	90 000
3 μm	30 cm	50 000	50 cm	150 000
1.5 μm	15 cm	33 000	50 cm	210 000

Table 1 gives an overview of the achievable plate numbers with CEC on the basis of the practical constraints mentioned above and an analysis time of 25 min.

3. Experimental

3.1. Chemicals

The buffers used were trishydroxymethylaminomethane (Tris), 2-morpholinoethanesulfonic acid (MES), sodium acetate (NaOAc) and phosphoric acid (H_3PO_4) all E. Merck, Darmstadt, Germany. All buffers were adjusted to the desired pH using either HCl or NaOH (E. Merck). The solvent used were acetonitrile, methanol and tetrahydrofuran, all J.T. Baker, Deventer, Netherlands. The eluents were prepared by first adjusting the buffer to the desired pH then mixing with the appropriate amount of organic modifier. The sample compounds were thiourea (E. Merck, Darmstadt, Germany), methyl-4-hydroxybenzoate, ethyl-4-hydroxybenzoate, propyl-4-hydroxybenzoate (synthes-

ized in house), butyl-4-hydroxybenzoate (Fluka, Buchs, Switzerland), pentyl-4-hydroxybenzoate (synthesized in house), naphthalene (E. Merck), biphenyl (E. Merck, Darmstadt, Germany), fluorene (Chem Service, Media, PA, USA), anthracene (E. Merck), phenanthrene (Chem Service), fluoranthene (Chem Service), Samples were prepared by mixing the appropriate buffer with a stock solution of 20 mg per compound in 100 ml acetonitrile to the same acetonitrile–buffer ratio as the respective eluent.

3.2. Columns

The capillaries were packed according to a slurry packing procedure described in detail in LC·GC magazine [18]. Polyimide coated fused-silica tubing was obtained from Polymicro (Phoenix, AZ, USA) with 100 μm I.D. and 350 μm O.D. Packed bed lengths of 25 cm and 40 cm were prepared, total column length was 8.5 cm plus packed bed length. Packing materials were obtained from Hypersil, Runcorn, UK (CEC Hypersil C_{18} 3 μm, ODS Hypersil 3 μm, BDS-ODS Hypersil 3 μm) and Phase Separation, Clwyd, UK (Spherisorb ODS I 3 μm, Spherisorb ODS II 3 μm).

3.3. Instrumentation

All CEC chromatograms were obtained with the HP HP^{3D}CE (Hewlett-Packard, Waldbronn, Germany) instrument modified so that pressure of 10–12 bar could be applied to the outlet and/or inlet vial. The pressurization of the columns was necessary to prevent formation of gas bubbles in the capillaries. After packing, columns were directly put into the HP^{3D}CE instrument and flushed with the run buffer electroosmotically for ca. 30 min before the first run. Changing eluents was also done electroosmotically. In the rare case that parts of a column had dried out, this column was purged on a HP 1050 pump CE (Hewlett-Packard) for ca. 30 min, this time was usually sufficient to remove all air bubbles from the column. Samples were injected electrokinetically (5 V for 3 s). The detection wavelength was at 250 nm.

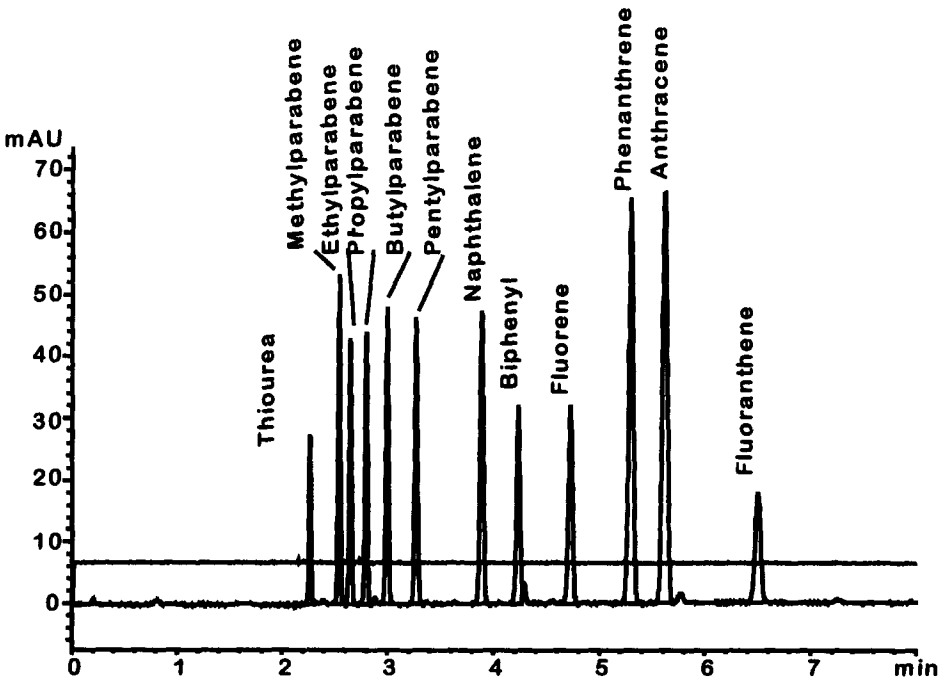

Fig. 6. Separation of a model mixture containing 5 parabenes, 6 PAHs and thiourea as t_0 marker. Conditions: 250(335) mm×0.1 mm CEC Hypersil C_{18}, 2.5 μm, acetonitrile–MES 25 m*M* pH 6 (80:20), 20 kV, 10 bar pressure applied to both ends of capillary, 20°C. Plate numbers 60 000–77 000.

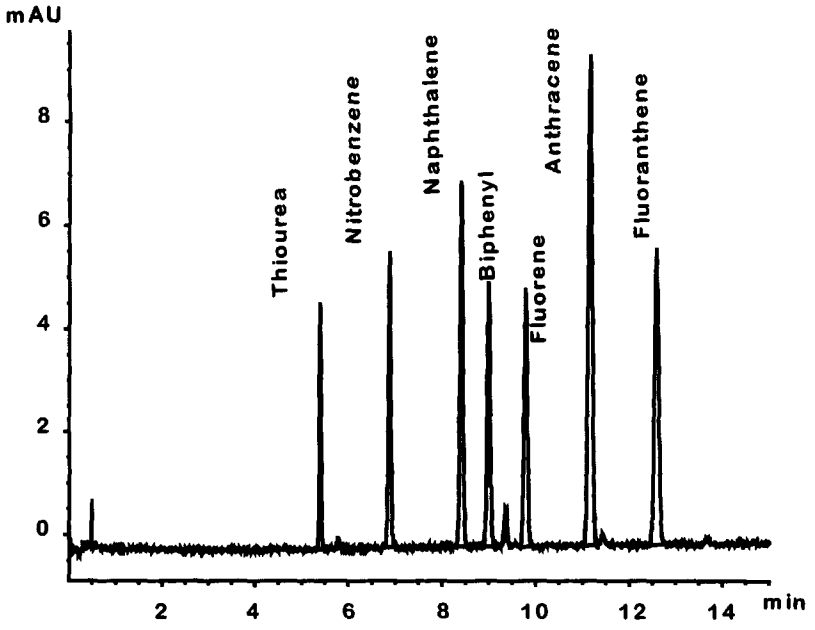

Fig. 7. Separation of a model mixture containing 6 PAHs and thiourea as t_0 marker. Conditions: 400(485) mm×0.1 mm Spherisorb ODS I, 3 μm, acetonitrile–MES 25 m*M* pH 6 (80:20), 30 kV, 10 bar pressure applied to both ends of capillary, 20°C. Plate numbers 90 000–100 000.

4. Results and discussion

Fig. 6 shows a separation of parabenes and PAHs on a capillary packed with CEC Hypersil C_{18}, 2.5 (L_{eff} = 25 cm, L_{tot} = 33.5 cm, I.D. = 0.1 mm) at 20°C, with acetonitrile–MES 25 m*M* pH 6 (80:20), 30 kV, The linear flow velocity under these conditions is 1.9 mm/s. The efficiencies for the single peaks are given in Table 2 (all plate numbers were calculated using the halfwidth method). The plate numbers on this column (ca. 70 000 plates on 25 cm) are comparable to our theoretical estimate for a 3 μm material

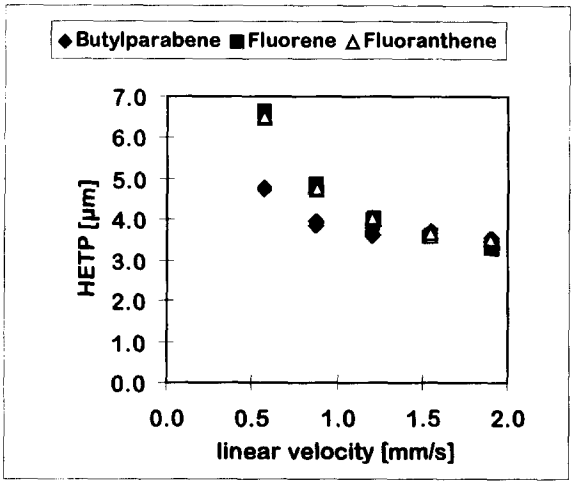

Fig. 8. *H–u* curves for Butylparabene, Fluorene and Fluoranthene. Conditions: 250(335) mm×0.1 mm CEC Hypersil C_{18}, 2.5 μm, acetonitrile–MES 25 m*M* pH 6 (80:20), 10 bar pressure applied to both ends of capillary, 20°C.

Table 2
Plates achieved in practice on a column packed with CEC Hypersil C_{18}, 2.5 μm (L_{eff} = 25 cm, L_{tot} = 33.5 cm, I.D. = 0.1 mm), with acetonitrile–MES 25 m*M* pH 6 (80:20), 30 kV, 20°C

Compound	Plates
Thiourea	60 600
Methylparabene	69 000
Ethylparabene	69 700
Propylparabene	71 000
Butylparabene	72 200
Pentylparabene	69 600
Naphthalene	62 300
Biphenyl	77 300
Fluorene	75 700
Phenanthrene	71 400
Anthracene	65 400
Fluoranthene	72 900

(150 000 plates on 50 cm). Using the values for ϵ_r (45) and η (0.55 cP) given in [21] for a 80:20 mixture of acetonitrile–water we calculate a ζ potential of 30 mV from the flow velocity of 1.9 mm/s.

Separation of PAHs on a column with a packed bed of 40 cm is shown in Fig. 7 (Spherisorb ODS I, 3 μm, L_{eff}=40 cm, L_{tot}=50 cm, I.D.=0.1 mm, acetonitrile–Tris·HCl 50 m*M* pH 8 (80:20), 30 kV, 20°C, flow velocity is 1.2 mm/s). On this column plate numbers of up to 100 000 are achieved. Using the values given above we calculate also for this phase under the given conditions a ζ potential of 30 mV.

Fig. 8 shows *H*–*u* curves for butylparabene (k'= 0.3), fluorene (k'=1.1) and fluoranthene (k'=1.9) obtained on a capillary packed with CEC Hypersil C_{18} 2.5 μm (I.D. 100 μm, packed bed length 25 cm). At flow velocities around 2 mm/s an HETP value of 3.3 is achieved for all three compounds which corresponds to a reduced plate height of 1.3. The HETP values for the parabene (as also for the other parabenes in the sample) are lower than those for the PAHs at low linear flow-rates. The reason for this behavior is unclear as the diffusion coefficients should be similar. In previous experiments [18] the opposite behavior has been observed (the parabenes having lower efficiencies than the PAHs).

Separation of a sample of PAHs on five different C_{18} stationary phases are shown in Fig. 9. All stationary phase particles were 3 μm, all columns were 25 cm packed bed (33.5 cm total length). Conditions were acetonitrile–Tris·HCl 50 m*M* pH 8 (80:20), 20 kV, 20°C. We see that the phases differ in retention properties as well as in EOF velocities under these conditions. The phases have been evaluated with different samples but thiourea (1), naphthalene (2), biphenyl, fluorene, anthracene and fluoranthene (3) were contained in all samples. Thiourea has been used throughout our investigation as the t_0 marker. CEC Hypersil C_{18} and Spherisorb ODS I which are both non-endcapped materials produce the fastest flow. The three phases from Hypersil have similar retention properties although the EOF velocities they produce are very different. The CEC Hypersil is a non-endcapped material and has the largest number of residual silanol groups. ODS Hypersil with less residual silanols show considerably slower flow. The BDS-ODS Hypersil is a base deactivated material which has a minimum number of residual silanol groups. This is reflected in the very low EOF flow-rate. The two Spherisorb phases have similar EOF but differ largely in retention properties. Table 3 gives the k' values for some of the compounds and the linear flow velocity on all five phases. The strong correlation of phase properties with EOF flow behavior supports the

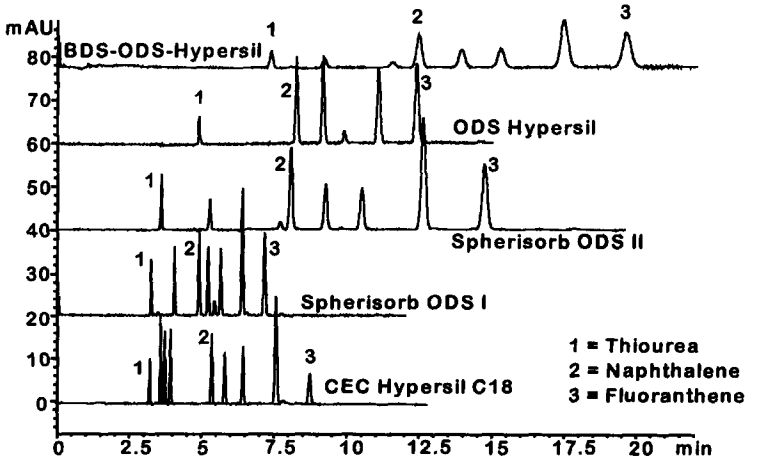

Fig. 9. Separation of PAHs on five reversed-phase C_{18} stationary phases. Conditions: 250(335) mm×0.1 mm, 3 μm, acetonitrile–Tris·HCl 50 m*M* pH 8 (80:20), 20 kV, 10 bar pressure applied to both ends of capillary, 20°C. Samples were not identical but all contained thiourea, naphthalene and fluoranthene.

Table 3
k' values and EOF velocity on five C_{18} 3 μm stationary phases

Stationary Phase	k'					EOF Velocity(mm/s)
	Naphthalene	Biphenyl	Fluorene	Anthracene	Fluoranthene	
CEC Hypersil C_{18}	0.67	0.81	1.01	1.36	1.72	1.35
ODS Hypersil	0.68	0.87	1.02	1.26	1.52	0.88
BDS-ODS Hypersil	0.69	0.89	1.07	1.37	1.66	0.59
Spherisorb ODS I	0.52	0.61	0.75	0.98	1.22	1.35
Spherisorb ODS II	1.11	1.40	1.71	2.24	2.76	1.07

All columns were 25 cm packed bed (33.5 cm total length). Conditions were: acetonitrile–Tris·HCl 50 m*M* pH 8 (80:20), 20 kV, 20°C.

assumption that the EOF in a packed capillary is mainly generated from the packing particles and not from the capillary wall.

To investigate the effect of pH and solvent composition on EOF velocity, the electrophoretic eluent mobilities on different stationary phases were determined as a function of pH and solvent composition. The mobility μ_e of an eluent is given by

$$\mu_e = \frac{\epsilon_0 \epsilon_r \zeta}{\eta} = \frac{u_e}{E} \quad (8)$$

The mobility μ_e has the dimensions [cm^2/V s] and is independent on the field strength. Flow velocities u_e were determined from the elution time of thiourea as t_0 marker.

Fig. 10 shows the eluent mobilities of mixtures 80% acteonitrile with buffers of different pH. The eluents were prepared such that the buffer was prepared and adjusted to the desired pH then mixed with acetonitrile. The x-axis in Fig. 10 represent the pH of the buffer prior to mixing, not the apparent pH after mixing with acetonitrile. The buffers were Tris·HCl 50 m*M* for pH 10.2, 9 and 8, MES 50 m*M* for pH 6, NaOAc 50 m*M* for pH 4 and H_3PO_4 for pH 1.8. Spherisorb ODS I was investigated in the pH range from 4 to 10.2, CEC Hypersil C_{18} in the range 1.8 to 8, ODS Hypersil at 8 and 8.8, Spherisorb ODS II and BDS-ODS Hypersil at pH 8.

We see a strong dependence of μ_e on pH in the range between 1.8 and 8 as can be expected from the

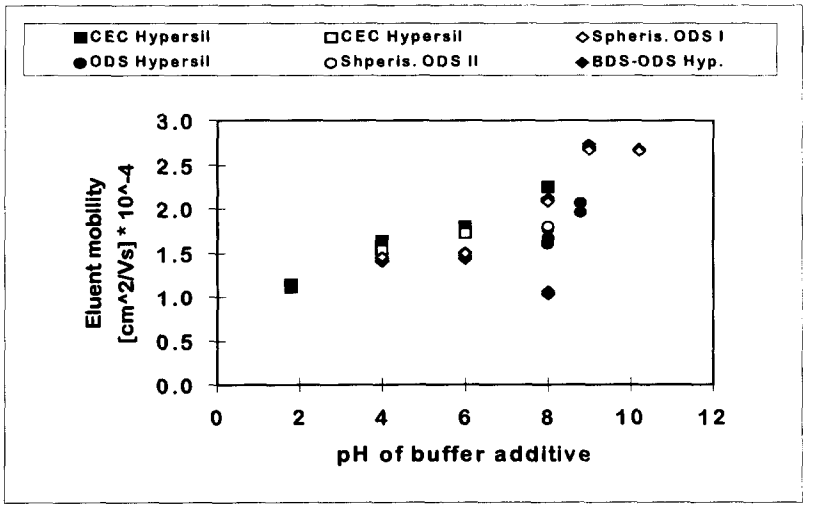

Fig. 10. Plots of eluent mobility vs. pH of buffer additive for various C_{18} stationary phases. Conditions acetonitrile–buffer (80:20), 571 V/cm, 10 bar pressure applied to both ends of capillary, 20°C. The buffers were Tris·HCl for pH 8, 8.8, 9 and 10.2, MES for pH 6, NaOAc for pH 4 and H_2PO_4 for pH 1.8, all buffer concentrations were 50 m*M*. The x-axis represents the pH of the buffer prior to mixing with acetonitrile.

changes in the degree of dissociation of the surface silanols in this pH range. No change was observed in going from pH 9 to pH 10.2 probably because at a pH above 9 the silanols are fully dissociated. Surprisingly, however a considerable EOF was observed at pH 1.8 where no surface charges due to dissociated silanols are supposed to be present. Compared to pH dependencies of EOF in untreated FS, pH typically ranges between $6 \cdot 10^{-4}$ $cm^2/V\,s$ (pH 10) and $0.25 \cdot 10^{-4}$ $cm^2/V\,s$ (pH 3) in aqueous systems [19,21]. In the case of C_{18} coated particles the EOF mobility only changes from ca. $1 \cdot 10^{-4}$ $cm^2/V\,s$ (pH 2) to $3 \cdot 10^{-4}$ $cm^2/V\,s$ (pH 10).

Fig. 11 shows the dependency of eluent mobility on organic modifier content, on CEC Hypersil C_{18} 3 μm (top) and Spherisorb ODS I 3 μm (bottom). Mobilities were determined from the elution time of thiourea at two different pHs (8 and 6) and two different buffer concentrations (50 mM and 25 mM). In all cases the eluent mobility increases with increasing acetonitrile content. In the literature different dependencies of eluent mobility on organic modifier content has been observed. Behnke et al. [12] observed an increase in mobility with increasing ACN content using a 2.5 mM pH 4 phosphate buffer. Yamamoto et al. [4] and Yan et al. [5] observed a decrease of mobility with increasing ACN content in a 4 mM pH 9 tetraborate buffer. Rebscher and Pyell [6] report an increase of mobility with increasing ACN content (2 mM tetraborate buffer pH not given). The reason for these contradicting observations is not clear.

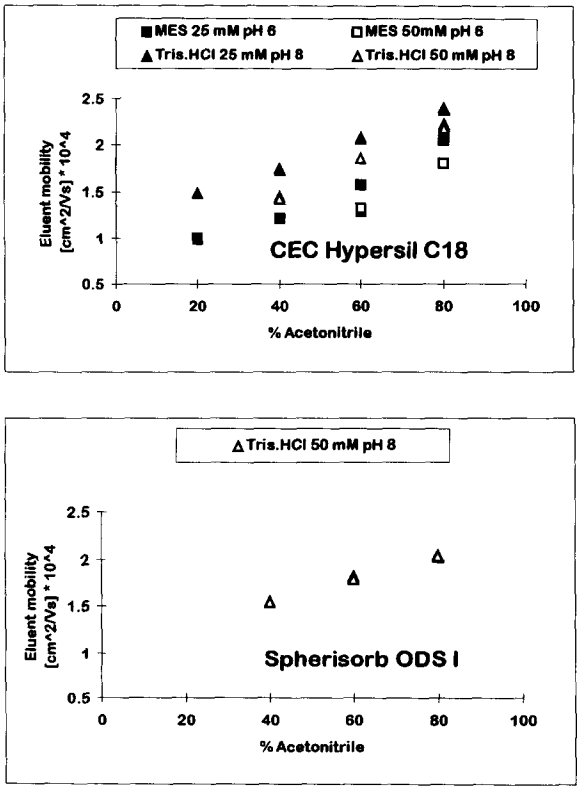

Fig. 11. Plots of eluent mobility vs. acetonitrile content for (top) CEC Hypersil C_{18} and (bottom) Spherisorb ODS I for different pH values and buffer concentrations. pH values given are those of buffer prior to mixing with acetonitrile.

Data from Schwer and Kenndler [21] indicate that in open fused-silica tubes the eluent mobility also decreases with increasing ACN content. Taking only the changes in bulk properties (viscosity and dielectric constant) into account the behavior should be vice versa. They concluded that the ζ potential itself changes, either by variation of the dielectric constant in the double layer or by a change in adsorption of potential determining ions upon addition of organic modifier.

In Fig. 12 a comparison of the separation of a test sample in acetonitrile–buffer (80:20) is compared to separation of the same sample in methanol–buffer (90:10). It is known from LC that these solvent compositions have comparable elution strength. The buffer was in both cases Tris·HCl 50 mM pH 8. The chromatogram with methanol–buffer was taken at 30 kV and 40°C, because the EOF flow at 20°C was very slow. The eluent mobility in the methanol–buffer (90:10) system was $0.3 \cdot 10^{-4}$ $cm^2/V\,s$ at 20°C and $0.48 \cdot 10^{-4}$ $cm^2/V\,s$ at 40°C compared to $2.1 \cdot 10^{-4}$ $cm^2/V\,s$ at 20°C for the acetonitrile–buffer (80:20) system.

This drastic reduction in EOF cannot be caused just by the change in dielectric constant and viscosity. The ratio of ϵ/η for an ACN–water (80:20) mixture is 82 cP^{-1} and for the methanol–water (90:10) mixture 47 cP^{-1}. This would account for a change in eluent mobility by a factor of ca. 2. We observe however a reduction in mobility by a factor of 7. This means that the ζ potential is altered drastically when changing from acetonitrile to methanol.

A similar effect has been observed when changing

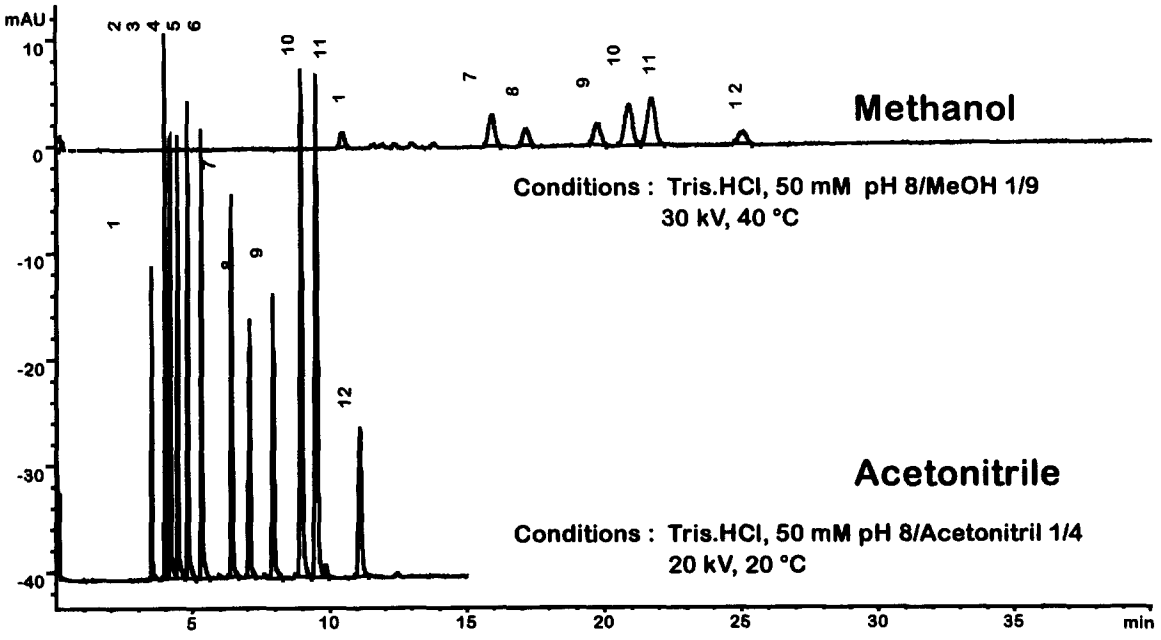

Fig. 12. Effect of changing from acetonitrile to methanol as organic modifier.

to THF as organic modifier (Fig. 13). The eluent mobility of the THF buffer system is $0.6 \cdot 10^{-4}$ $cm^2/V\,s$ at 20°C.

In the attempt to separate our test sample with methanol we made the observation that the peak areas of the parabenes are reduced with respect to the

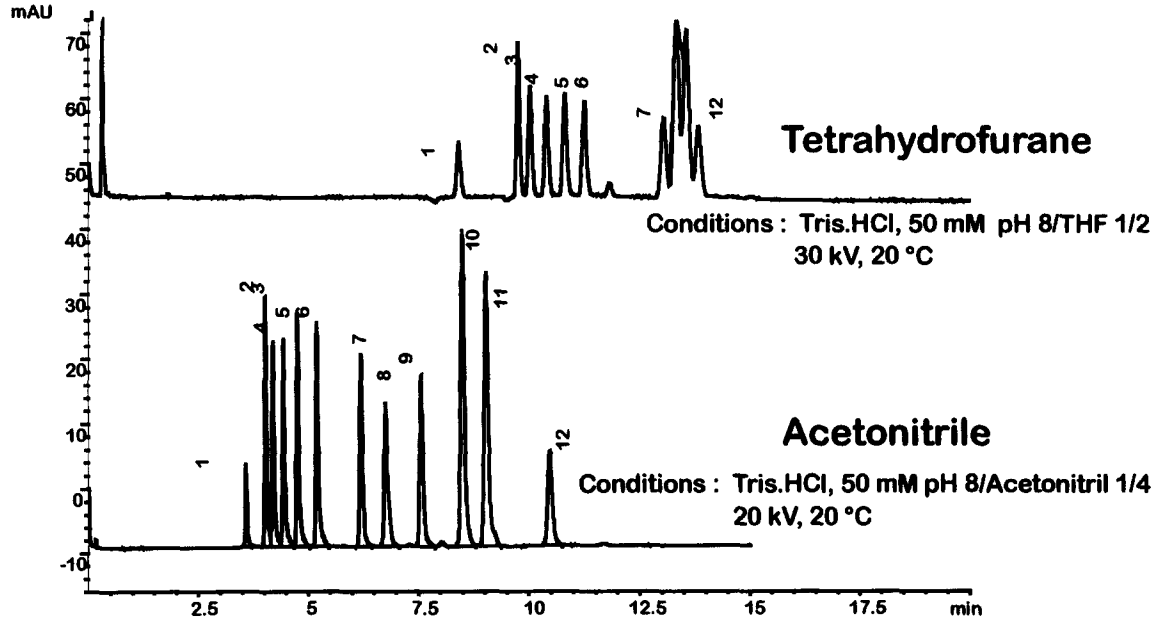

Fig. 13. Effect of changing from acetonitrile to tetrahydrofurane as organic modifier.

other components. In the separation with THF the resolution of the PAHs is very poor compared to that of the parabenes. These effects need further elucidation.

5. Conclusions

We believe that capillary electrochromatography is on the verge of becoming an important complementary capillary separation technique because it combines the best properties of CE viz. separation efficiency, with the best properties of HPLC viz. control of retention and selectivity. The implementation of the technique described here, reversed-phase separation of neutral solutes is easily executed on a modified commercially available CE instrument. The efficiency and EOF velocity predicted in our model can be achieved in practice.

But this work also shows that there are still a number of questions that need to be addressed in future work. Careful studies of the influence of operational parameters like solvent composition, pH, ion strength must lead to simple models that allow easy selection of starting conditions and optimization of separation.

References

[1] V. Pretorius, B.J. Hopkins and J.D. Schieke, J. Chromatogr., 99 (1974) 23.
[2] J.H. Knox and I.H. Grant, Chromatographia, 24 (1987) 135.
[3] J.H. Knox and I.H. Grant, Chromatographia 32, (1991) 317.
[4] H. Yamamoto, H. Baumann and F. Erni, J. Chromatogr., 593 (1992) 313.
[5] C. Yan, D. Schaufelberger and F. Erni, J. Chromatogr. A, 670 (1994) 15.
[6] H. Rebscher and U. Pyell, Chromatographia, 38 (1994) 737.
[7] N.W. Smith and M.B. Evans, Chromatographia, 38 (1994) 649.
[8] N.W. Smith and M.B. Evans, Chromatographia, 41 (1995) 197.
[9] R.J. Boughtflower, T. Underwood and C.J. Paterson, Chromatographia, 40 (1995) 329.
[10] R.J. Boughtflower, T. Underwood and J. Maddin, Chromatographia, 41 (1995) 398.
[11] K.K. Unger and T. Eimer, Fresenius' Z. Anal. Chem., 352 (1995) 649.
[12] B.Behnke and E. Bayer, J. Chromatogr. A, 680 (1994) 93.
[13] T. Tsuda, LC·GC Int., 5 (1992) 26.
[14] C. Yan, R. Dadoo, H. Zhao and R.N. Zare, Anal. Chem., 67 (1995) 2026.
[15] Robert J. Hunter, Zeta Potential in Colloid Science, Academic Press, London, 1981, Ch. 2.
[16] Cs. Horvath and H.-J. Lin, J. Chromatogr., 126 (1976) 401.
[17] Cs. Horvath and H.-J. Lin, J. Chromatogr., 149 (1978) 43.
[18] M.M. Dittmann and G.P. Rozing, LC·GC, 13 (1995) 800.
[19] K. Shoiket, H. Bayer, T. Schmitt and H. Engelhardt, Poster presented at the HPCE '95, Würzburg, 29.1-2.2, 1995.
[20] W. Schützner and E. Kenndler, Anal. Chem., 64 (1992) 1991.
[21] Ch. Schwer and E. Kenndler, Anal. Chem., 64 (1991) 1801.